Potential for Redox Isomerism by Quinone Complexes of Iron(III). Studies on Complexes of the Fe^{III}(N-N)(DBSQ)(DBCat) Series with 2,2′-Bipyridine and *N*,*N*,*N*′,*N*′-Tetramethylethylenediamine Coligands

Attia S. Attia,[†] Samaresh Bhattacharya,[‡] and Cortlandt G. Pierpont*

Department of Chemistry and Biochemistry, University of Colorado, Boulder, Colorado 80309

Received February 9, 1995[⊗]

Iron complexes of the Fe^{III}(N-N)(DBSQ)(DBCat) series, where N-N = bpy, tmeda, and DBSQ and DBCat are semiquinonate and catecholate ligands derived from 3,5- and 3,6-di-*tert*-butyl-1,2-benzoquinone, have been investigated to assess the potential for isomerism to Fe^{II}(N-N)$(DBSQ)_2$ species in the manner of related complexes of Mn and Co. Crystallographic characterization is provided for Fe(bpy)(3,6-DBSQ)(3,6-DBCat) [monoclinic, $C2/c$, a = 10.809(1) Å, b = 30.149(6) Å, c = 12.275(2) Å, β = 114.52(1)°, and Z = 4], Fe(tmeda)(3,6-DBSQ)-(3,6-DBCat) [monoclinic, $P2_1/c$, a = 14.531(3) Å, b = 13.328(3) Å, c = 19.781(3) Å, β = 106.63(2)°, and Z = 4], and Fe(tmeda)(3,5-DBSQ)(3,5-DBCat)·$2C_3H_5OH$ [monoclinic, $P2_1/n$, a = 11.884(2) Å, b = 14.856(2) Å, c = 25.115(5) Å, β = 93.15(2)°, and Z = 4]. All three complex molecules are monomeric and octahedral. Intermolecular stacking for Fe(bpy)(3,6-DBSQ)(3,6-DBCat) appears responsible for an anomalous drop in magnetic moment at low temperature; the complexes containing tmeda ligands have S = 2 magnetic moments that result from strong Fe(III)−semiquinone radical antiferromagnetic exchange. Electronic spectra of all three complexes show strong solvatochromic effects, little temperature dependence, and no bands in the infrared that appear characteristically for related Co(III) and Mn(III) complexes that exhibit redox isomerism. The absence of isomerism for the iron complexes is explained in terms of thermodynamic changes that contribute to equilibria of the Co-(N-N)$(DBQ)_2$ and Mn(N-N)$(DBQ)_2$ series.

Introduction

Many of the unique and interesting properties of transition metal complexes containing quinone ligands arise from the similarity in energy between the redox-active quinone electronic levels and the metal d orbitals.[1] In most complexes charge distribution remains discrete with little metal−ligand delocalization and well-defined charges for the metal ion and the coordinated semiquinonate and catecholate ligands. In a few unique cases the balance of metal and quinone orbital energies is such that temperature-dependent shifts in charge distribution may be observed under equilibrium conditions.[2,3] These equilibria are essentially metal−quinone electron transfer reactions that are not dissimilar from the photoexcitation of $[Ru^{II}(bpy)_3]^{2+}$ to give the charge-separated $[Ru^{III}(bpy)_2(bpy^{\bullet-})]^{2+}$ redox isomer. A notable difference is that the energy separation between metal and quinone levels is in the infrared rather than the UV or visible region. Redox isomerism has been observed to occur most commonly for two classes of quinone complexes. In 1980 we reported the equilibrium between Co(III) and Co(II) redox isomers of a complex containing semiquinonate (SQ) and catecholate (Cat) ligands derived from 3,5-di-*tert*-butyl-1,2-benzoquinone (3,5-DBBQ):[2a]

$$Co^{III}(bpy)(3,5\text{-}DBSQ)(3,5\text{-}DBCat) \rightleftarrows Co^{II}(bpy)(3,5\text{-}DBSQ)_2 \quad (1)$$

In more recent research we and others have extended these studies to related complexes of Co containing other N-donor coligands and to complexes prepared with 3,6-DBBQ.[2] Equilibria occur in separate electron transfer (eq 2) and spin transition (eq 3)

$$\underset{(d\pi)^6(d\sigma)^0(\pi_{Q1})^2(\pi_{Q2})^1}{Co^{III}(N\text{-}N)(SQ)(Cat)} \rightleftarrows \underset{(d\pi)^6(d\sigma)^1(\pi_{Q1})^1(\pi_{Q2})^1}{Co^{II}(N\text{-}N)(SQ)_2} \quad (2)$$

$$\underset{(d\pi)^6(d\sigma)^1(\pi_{Q1})^1(\pi_{Q2})^1}{Co^{II}(N\text{-}N)(SQ)_2} \rightleftarrows \underset{(d\pi)^5(d\sigma)^2(\pi_{Q1})^1(\pi_{Q2})^1}{Co^{II}(N\text{-}N)(SQ)_2} \quad (3)$$

steps that give a high-spin Co(II) isomer.[3,4] The second class of complexes that show redox isomeric equilibria are the compounds of Mn that are related to the Co series.[3] In this case electron transfer occurs in two one-electron steps that involve Mn(IV), high-spin Mn(III), and high-spin Mn(II) redox isomers:

$$\underset{(d\pi)^3(d\sigma)^0(\pi_{Q1})^2(\pi_{Q2})^2}{Mn^{IV}(N\text{-}N)(Cat)_2} \rightleftarrows \underset{(d\pi)^3(d\sigma)^1(\pi_{Q1})^2(\pi_{Q2})^1}{Mn^{III}(N\text{-}N)(SQ)(Cat)} \quad (4)$$

$$\underset{(d\pi)^3(d\sigma)^1(\pi_{Q1})^2(\pi_{Q2})^1}{Mn^{III}(N\text{-}N)(SQ)(Cat)} \rightleftarrows \underset{(d\pi)^3(d\sigma)^2(\pi_{Q1})^1(\pi_{Q2})^1}{Mn^{II}(N\text{-}N)(SQ)_2} \quad (5)$$

[†] Present address: Ain Shams University, Cairo, Egypt.
[‡] Present address: Jadavpur University, Calcutta, India.
[⊗] Abstract published in *Advance ACS Abstracts,* July 15, 1995.

(1) (a) Pierpont, C. G.; Buchanan, R. M. *Coord. Chem. Rev.* **1981**, *38*, 45. (b) Pierpont, C. G.; Lange, C. W. *Prog. Inorg. Chem.* **1993**, *41*, 381.
(2) (a) Buchanan, R. M.; Pierpont, C. G. *J. Am. Chem. Soc.* **1980**, *102*, 4951. (b) Abakumov, G. A.; Cherkasov, V. K.; Bubnov, M. P.; Ellert, O. G.; Dobrokhotova, Z. B.; Zakharov, L. N.; Struchkov, Y. T. *Dokl. Akad. Nauk SSSR* **1993**, *328*, 12. (c) Adams, D. M.; Dei, A.; Rheingold, A. L.; Hendrickson, D. N. *J. Am. Chem. Soc.* **1993**, *115*, 8221. (d) Jung, O.-S.; Pierpont, C. G. *J. Am. Chem. Soc.* **1994**, *116*, 1127. (e) Jung, O.-S.; Pierpont, C. G. *Inorg. Chem.* **1994**, *33*, 2227.
(3) (a) Lynch, M. W.; Hendrickson, D. N.; Fitzgerald, B. J.; Pierpont, C. G. *J. Am. Chem. Soc.* **1984**, *106*, 2041. (b) Attia, A. S.; Pierpont, C. G. *Inorg. Chem.* **1995**, *34*, 1172.
(4) Pierpont, C. G.; Jung, O.-S. *Inorg. Chem.*, in press.

0020-1669/95/1334-4427$09.00/0 © 1995 American Chemical Society

Table 1. Crystallographic Data for Fe(bpy)(3,6-DBSQ)(3,6-DBCat), Fe(tmeda)(3,6-DBSQ)(3,6-DBCat), and Fe(tmeda)(3,5-DBSQ)(3,5-DBCat)[a]

	Fe(bpy)(3,6-DBSQ)(3,6-DBCat)	Fe(tmeda)(3,6-DBSQ)(3,6-DBCat)	Fe(tmeda)(3,5-DBSQ)(3,5-DBCat)·2C_3H_5OH
formula	$C_{38}H_{48}N_2O_4Fe$	$C_{34}H_{56}N_2O_4Fe$	$C_{40}H_{72}N_2O_6Fe$
fw	652.6	612.7	732.8
color	dark blue	violet	blue
space group	*C2/c*	$P2_1/c$	$P2_1/n$
a, Å	10.809(1)	14.531(3)	11.884(2)
b, Å	30.149(6)	13.328(3)	14.856(2)
c, Å	12.275(2)	19.781(3)	25.115(5)
β, deg	114.52(1)	106.63(2)	93.15(2)
V, Å^3	3639(1)	3671(1)	4427(1)
Z	4	4	4
T, °C	24	24	24
λ(Mo Kα), Å	0.710 73	0.710 73	0.710 73
D_{calcd}, g cm^{-3}	1.191	1.109	1.099
μ, mm^{-1}	0.450	0.442	0.379
R, R_w	0.044, 0.057	0.075, 0.076	0.064, 0.071

[a] $R = \sum||F_o| - |F_c||/\sum|F_o|$. $R_w = [\sum w(|F_o| - |F_c|)^2/\sum w(F_o)^2]^{1/2}$.

Equilibrium measurements on Co(bpy)(3,5-DBSQ)(3,5-DBCat) recorded in solution and in the solid state have provided thermodynamic parameters that are in close agreement with values for intramolecular enthalpy and entropy changes associated with Co(III/II) redox reactions.[5] Population of the antibonding dσ orbital in both Co and Mn equilibria results in a relatively large enthalpic increase. Associated low-energy shifts in vibrational modes with increases in complex spin degeneracy and structural flexibility give a large, positive entropy change that is responsible for the strong temperature dependence of the equilibria.[5a] Iron, the element between Mn and Co in the first transition series, appears not to undergo redox isomerism (eq 6), although complexes of Fe that are strictly analogous to

$$Fe^{III}(N\text{-}N)(SQ)(Cat) \rightleftharpoons Fe^{II}(bpy)(SQ)_2 \qquad (6)$$

complexes of Co and Mn that show isomerism have not been studied until recently.[6] Hendrickson reported Fe^{III}(bpy)(3,5-DBSQ)(3,5-DBCat) in 1982 but concluded from spectroscopic and magnetic characterization that the complex was oligomeric.[7] Bridged structures are not uncommon among complexes containing ligands derived from 3,5-DBBQ due to the exposed oxygen atom at the ring 1-position of 3,5-DBSQ and 3,5-DBCat. Tetrameric [Fe^{III}(3,5-DBSQ)(3,5-DBCat)]$_4$ is a relevant example of such bridging.[8] Semiquinone and catecholate ligands derived from 3,6-DBBQ have *tert*-butyl substituents blocking both oxygen sites, and these ligands form complexes with simple chelated structures. We now report the results of studies on iron complexes containing quinone ligands derived from both 3,5-DBBQ and 3,6-DBBQ. Nitrogen-donor coligands have been chosen to give compounds that are directly related to complexes of both Co and Mn that show isomeric equilibria with the objective of investigating the potential for redox isomerism by related complexes of iron.

Experimental Section

Materials. 2,2′-Bipyridine (bpy), *N,N,N′,N′*-tetramethylethylenediamine (tmeda), and 3,5-di-*tert*-butyl-1,2-benzoquinone were purchased from Aldrich. Iron pentacarbonyl was purchased from Strem Chemical Co. 3,6-Di-*tert*-butyl-1,2-benzoquinone (3,6-DBBQ) and Fe(3,6-DBSQ)$_3$ were prepared using literature procedures.[9,10]

Complex Syntheses. Fe(bpy)(3,6-DBSQ)(3,6-DBCat). Fe(3,6-DBSQ)$_3$ (0.23 g, 0.32 mmol) and bpy (0.06 g, 0.46 mmol) were dissolved in 60 mL of degassed hexane under N_2. The dark blue microcrystalline product precipitated from solution over a period of 2 h. It was separated from the solution by filtration in greater than 85% yield and washed with cold hexane. Crystals suitable for crystallographic analysis were obtained by recrystallization from a dichloromethane/hexane solution.

Anal. Calc for $C_{38}H_{48}N_2O_4Fe$: C, 70.0; H, 7.4; N, 4.3. Found: C, 70.3; H, 7.5; N, 4.0.

Fe(tmeda)(3,6-DBSQ)(3,6-DBCat). 3,6-DBBQ (0.05 g, 0.23 mmol) and tmeda (0.12 g, 1.14 mmol) were dissolved in 30 mL of degassed toluene. The mixture was added to $Fe(CO)_5$ (0.15 mL, 1.47 mmol) under N_2, and the solution was irradiated with a Hg lamp for a period of 1 h. During irradiation the color of the solution became deep violet. The volume of the solution was reduced under vacuum, and the crude product was obtained as a violet solid. Recrystallization from a toluene/2-propanol mixture gave crystals suitable for crystallographic analysis in 58% yield.

Anal. Calc for $C_{34}H_{56}N_2O_4Fe$: C, 66.2; H, 9.1; N, 4.5. Found: C, 65.3; H, 8.8; N, 5.1.

Fe(tmeda)(3,5-DBSQ)(3,5-DBCat). The synthetic procedure described above for Fe(tmeda)(3,6-DBSQ)(3,6-DBCat) was followed to give the complex in 74% yield. Crystalline samples obtained by recrystallization from toluene/2-propanol were found to be solvated as Fe(tmeda)(3,5-DBSQ)(3,5-DBCat)·2C_3H_5OH.

Anal. Calc for $C_{40}H_{68}N_2O_4Fe$: C, 65.8; H, 9.3; N, 3.8. Found: C, 64.2; H, 8.6; N, 3.2.

Physical Measurements. Electronic spectra were recorded on a Perkin-Elmer Lambda 9 spectrophotometer equipped with an RMC-Cryosystems cryostat. Solid samples were prepared as KBr pellets. Magnetic measurements were made using a Quantum Design SQUID magnetometer at a field strength of 5 kG. Infrared spectra were recorded on a Perkin-Elmer 1600 FTIR instrument with samples prepared as KBr pellets. Cyclic voltammograms were obtained with a Cypress CYSY-1 computer-controlled electroanalysis system. A Ag/Ag^+ reference electrode was used that consisted of a CH_3CN solution of $AgPF_6$ in contact with a silver wire placed in glass tubing with a Vycor frit at one end to allow ion transport. Tetrabutylammonium hexafluorophosphate was used as the supporting electrolyte, and the Fc/Fc^+ couple was used as an internal standard. With this experimental arrangement the Fc/Fc^+ couple appeared at 0.206 V vs Ag/Ag^+ with ΔE = 162 mV without correction for cell *iR* drop.

Crystallographic Structure Determinations. Fe(bpy)(3,6-DBSQ)(3,6-DBCat). Dark blue prismatic crystals of the complex were obtained by recrystallization from a hexane/dichloromethane solution.

(5) (a) Richardson, D. E.; Sharpe, P. *Inorg. Chem.* **1991**, *30*, 1412. (b) Richardson, D. E.; Sharpe, P. *Inorg. Chem.* **1993**, *32*, 1809.
(6) Attia, A. S.; Jung, O.-S.; Pierpont, C. G. *Inorg. Chim. Acta* **1994**, *226*, 91.
(7) Lynch, M. W.; Valentine, M.; Hendrickson, D. N. *J. Am. Chem. Soc.* **1982**, *104*, 6982.
(8) Boone, S. R.; Purser, G. H.; Chang, H.-R.; Lowery, M. D.; Hendrickson, D. N.; Pierpont, C. G. *J. Am. Chem. Soc.* **1989**, *111*, 2292.
(9) Belostotskaya, I. S.; Komissarova, N. L.; Dzhuaryan, E. V.; Ershov, V. V. *Izv. Akad. Nauk SSSR* **1972**, 1594.
(10) Attia, A. S.; Pierpont, C. G. Submitted for publication.

Table 2. Selected Atom Coordinates ($\times 10^4$) for Fe(bpy)(3,6-DBSQ)(3,6-DBCat)

	x/a	*y/b*	*z/c*
Fe	5000	6678(1)	2500
O1	3735(3)	6258(1)	1343(2)
O2	5867(3)	6628(1)	1363(2)
N1	6307(4)	7249(1)	3119(3)
C1	4210(4)	6084(1)	618(3)
C2	5402(4)	6294(1)	622(3)
C3	5999(4)	6152(1)	−156(3)
C4	5371(4)	5796(1)	−865(3)
C5	4226(4)	5584(1)	−849(3)
C6	3611(4)	5714(1)	−133(3)
C15	7649(6)	7216(2)	3675(4)
C16	8483(7)	7579(2)	3957(5)
C17	7882(10)	7988(3)	3661(6)
C18	6544(9)	8020(2)	3084(5)
C19	5744(5)	7649(1)	2825(3)

Table 3. Selected Atom Coordinates ($\times 10^4$) for Fe(tmeda)(3,6-DBSQ)(3,6-DBCat)

	x/a	*y/b*	*z/c*
Fe	3106(1)	1892(2)	2178(1)
O1	1795(7)	1666(7)	2318(5)
O2	2637(9)	658(8)	1594(5)
C1	1288(15)	976(13)	1960(9)
C2	1793(15)	415(13)	1537(9)
C3	1297(17)	−389(17)	1125(11)
C4	395(19)	−577(14)	1144(10)
C5	−92(14)	−39(18)	1541(11)
C6	328(15)	774(15)	1952(9)
O3	2647(6)	2995(7)	1541(5)
O4	4212(6)	2010(7)	1840(4)
C15	3267(11)	3255(12)	1174(8)
C16	4127(11)	2697(11)	1348(7)
C17	4808(11)	2858(11)	984(7)
C18	4616(10)	3625(12)	499(7)
C19	3787(13)	4195(10)	346(7)
C20	3069(12)	4012(12)	675(8)
N1	3490(10)	2922(11)	3106(7)
N2	3960(10)	883(10)	3028(7)
C29	3917(14)	2346(13)	3744(8)
C30	4524(11)	1515(14)	3587(9)

Axial photographs indicated monoclinic symmetry, and the centered settings of 25 intense reflections with 2θ values between 17 and 25° gave the unit cell dimensions listed in Table 1. Data were collected by $\theta-2\theta$ scans within the angular range 3.0−50°. A Patterson map indicated that the metal atom was located on the 2-fold axis of the space group with $Z = 4$. Phases derived from the location of the Fe atom gave the positions of other atoms of the structure. Final cycles of refinement converged with discrepancy indices of $R = 0.044$ and $R_w = 0.057$. Selected atomic coordinates are listed in Table 2. Tables containing full listings of atom positions, anisotropic displacement parameters, and hydrogen atom locations are available as supplementary material.

Fe(tmeda)(3,6-DBSQ)(3,6-DBCat). Dark blue prismatic crystals of the complex were obtained by recrystallization from a toluene/2-propanol solution. Axial photographs showed that even relatively large crystals diffracted weakly. Photographs indicated monoclinic symmetry, and the centered settings of 25 intense reflections with 2θ values between 18 and 29° gave the unit cell dimensions listed in Table 1. Data were collected by $\theta-2\theta$ scans within the angular range 3.0−45°. A Patterson map was used to determine the coordinates of the Fe atom, and phases derived from the location of the Fe atom gave the positions of other atoms of the structure. Final cycles of refinement converged with discrepancy indices of $R = 0.075$ and $R_w = 0.076$. Selected atomic coordinates are listed in Table 3. Tables containing full listings of atom positions, anisotropic displacement parameters, and hydrogen atom locations are available as supplementary material.

Fe(tmeda)(3,5-DBSQ)(3,5-DBCat). Dark blue needles of the complex were obtained by recrystallization from a toluene/2-propanol solution. Axial photographs showed that even relatively large crystals diffracted weakly. Photographs indicated monoclinic symmetry, and

Table 4. Selected Atom Coordinates ($\times 10^4$) for Fe(tmeda)(3,5-DBSQ)(3,5-DBCat)

	x/a	*y/b*	*z/c*
Fe	3202(1)	1378(1)	2242(1)
O1	1649(6)	1129(5)	2386(3)
O2	3464(6)	1007(5)	2972(3)
C1	1512(10)	876(9)	2892(5)
C2	2520(9)	826(7)	3219(5)
C3	2470(10)	611(8)	3760(5)
C4	1398(12)	392(8)	3931(5)
C5	404(10)	424(8)	3614(5)
C6	481(10)	701(8)	3095(5)
O3	3624(6)	196(5)	1883(3)
O4	2802(6)	1648(6)	1450(3)
C15	3372(9)	180(8)	1374(5)
C16	2925(10)	989(9)	1139(5)
C17	2625(10)	1039(9)	575(5)
C18	2793(10)	257(10)	311(5)
C19	3239(10)	−573(9)	521(5)
C20	3533(9)	−587(8)	1055(5)
N1	5019(8)	1750(7)	2246(4)
N2	3068(9)	2847(7)	2377(4)
C29	5104(11)	2666(10)	2486(6)
C30	4164(11)	3234(9)	2284(6)

the centered settings of 25 intense reflections with 2θ values between 18 and 26° gave the unit cell dimensions listed in Table 1. Data were collected by $\theta-2\theta$ scans within the angular range 3.0−45°. A Patterson map was used to determine the coordinates of the Fe atom, and phases derived from the location of the Fe atom gave the positions of other atoms of the complex molecule. A subsequent difference Fourier map revealed the atomic positions of two independent 2-propanol solvate molecules. Final cycles of refinement converged with discrepancy indices of $R = 0.064$ and $R_w = 0.071$. Selected atomic coordinates are listed in Table 4. Tables containing full listings of atom positions, anisotropic displacement parameters, and hydrogen atom locations are available as supplementary material.

Results

Considerable interest has been directed at the possibility that catecholate complexes of iron(III) may show Cat → Fe electron transfer leading to stable semiquinone Fe(II) redox isomers.[11] The complexes of specific interest in this context are those that are directly analogous with compounds of Co and Mn that show redox isomerism. Complexes formed with 3,6-DBBQ typically have monomeric structures, in contrast to the bridged oligomers that are sometimes encountered with ligands derived from 3,5-DBBQ. We have consequently used 3,6-DBBQ in our synthetic procedures, as well as 3,5-DBBQ. Studies with Co and Mn have indicated that the choice of N-donor coligand is important in defining charge distribution. For example, bpy and tmeda have been found to give isomers of high oxidation state metal ions, $Co^{III}(N\text{-}N)(SQ)(Cat)$ and $Mn^{IV}(N\text{-}N)(Cat)_2$, while 5-nitro-1,10-phenanthroline gives the low oxidation state isomers $M^{II}(NO_2\text{-phen})(3,6\text{-DBSQ})_2$, M = Co, Mn. Synthetic procedures carried out with nitrophenanthroline and diazafluorenone gave only $Fe(3,6\text{-DBSQ})_3$ with 3,6-DBBQ and $Fe(3,5\text{-DBSQ})_3$/[Fe(3,5-DBSQ)(3,5-DBCat)]$_4$ mixtures with 3,5-DBBQ.[8] Consequently, the coligands included in this report are bpy and tmeda; the *trans* complexes of pyridine and 4-*tert*-butylpyridine have been reported separately.[6]

Fe(bpy)(3,6-DBSQ)(3,6-DBCat). Samples of dark blue Fe(bpy)(3,6-DBSQ)(3,6-DBCat) may be obtained in crystalline form by treating green $Fe(3,6\text{-DBSQ})_3$ with bipyridine. This is in contrast to similar reactions carried out with $Fe(3,5\text{-DBSQ})_3$

(11) (a) Hider, R. C.; Mohd-Nor, A. R.; Silver, J.; Morrison, I. E. G.; Rees, L. V. C. *J. Chem. Soc., Dalton Trans.* **1981**, 609. (b) Funabiki, T.; Kojima, H.; Kaneko, M.; Inoue, T.; Yoshioka, T.; Tanaka, T.; Yoshida, S. *Chem. Lett.* **1991**, 2143.

Table 5. Selected Bond Lengths (Å) for Members of the Fe(N-N)(DBSQ)(DBCat) Series

complex	$Fe-O_{Cat}$	$Fe-O_{SQ}$	Fe−N	$C-O_{Cat}$	$C-O_{SQ}$
Fe(bpy)(3,6-DBSQ)(3,6-DBCat)[a]	1.971(2), 1.984(2)		2.154(4)	1.307(5), 1.308(4)	
Fe(tmeda)(3,6-DBSQ)(3,6-DBCat)	1.916(10), 1.926(10)	2.014(10), 2.024(11)	2.231(14), 2.232(13)	1.34(2), 1.35(2)	1.25(2), 1.26(2)
Fe(tmeda)(3,5-DBSQ)(3,5-DBCat)	1.926(7), 1.936(8)	2.048(8), 2.057(8)	2.217(10), 2.228(10)	1.34(1), 1.34(1)	1.27(1), 1.29(1)
$Fe(Bupy)_2$(3,6-DBSQ)(3,6-DBCat)[a,b]	1.968(4), 1.973(5)		2.205(5)	1.307(8), 1.315(8)	

[a] Bond lengths for SQ and Cat ligands averaged by crystallographically imposed symmetry. [b] Reference 6.

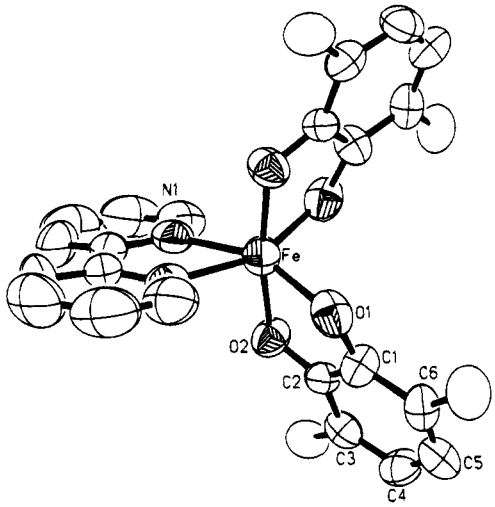

Figure 1. Drawing of Fe(bpy)(3,6-DBSQ)(3,6-DBCat) with *tert*-butyl methyl carbon atoms omitted.

that lead only to amorphous or microcrystalline powders.[7] Crystals of Fe(bpy)(3,6-DBSQ)(3,6-DBCat) have been found to be isomorphous with Co^{III}(bpy)(3,6-DBSQ)(3,6-DBCat) and Mn^{IV}(bpy)$(3,6\text{-DBCat})_2$, complexes that have been observed to undergo temperature-dependent redox isomerism in solution and in the solid state.[2b,3b] A drawing of the complex molecule is shown in Figure 1; selected bond lengths and angles are listed in Table 5. The iron atom is located on an axis of crystallographic 2-fold symmetry that transposes the dissimilar SQ and Cat ligands. Structural features of the quinone ligand are an average of values expected for separate SQ and Cat ligands. The C−O length is 1.308(4) Å, compared with the values of 1.311 Å for Co(bpy)(3,6-DBSQ)(3,6-DBCat) and 1.354(4) Å for Mn^{IV}(bpy)$(3,6\text{-DBCat})_2$. Bond lengths from the iron to the oxygen and nitrogen donor atoms are values that would be expected for Fe(III), and the Fe−O1 length at the site *trans* to the bpy nitrogen is slightly shorter (1.971(2) Å) than the value *trans* to the related quinone oxygen atom (1.984(3) Å). A feature of the crystal structure that was important in understanding the photomechanical properties of the Co analog was the formation of one-dimensional stacks of complex molecules linked by overlapped rings of bpy ligands of adjacent complex molecules. The crystal structure of Fe(bpy)(3,6-DBSQ)(3,6-DBCat) is the same, and this may be significant in understanding the magnetic properties of the complex.

Magnetic measurements were important in demonstrating redox equilibria for the Co(N-N)(SQ)(Cat) complexes in the solid state.[2] Complexes of Fe(III) containing chelated 3,5- and 3,6-DBSQ radical ligands have all been found to show strong antiferromagnetic coupling between metal $d\pi$ electrons and the radical spins.[8,10] Both $Fe(3,5\text{-DBSQ})_3$ and $Fe(3,6\text{-DBSQ})_3$ have $S = 1$ magnetic moments at temperatures above 300 K, and it may be anticipated that Fe−SQ exchange in the Fe(N-N)(DBSQ)(DBCat) species will be strong. The plot of μ_{eff} vs temperature for Fe(bpy)(3,6-DBSQ)(3,6-DBCat) is shown in Figure 2. At 350 K the magnetic moment is 5.64 μ_B and the low-temperature value at 5 K is 0.81 μ_B. This is quite similar to the behavior observed by Hendrickson for Fe(bpy)(3,5-DBSQ)(3,5-DBCat) and Fe(phen)(3,5-DBSQ)(3,5-DBCat).[7] Values for magnetic moment at the high end of the temperature range are greater than 4.90 μ_B for a strongly coupled $S = 2$ molecule but less than the 6.16 μ_b weak exchange limit. A shift in charge distribution to a high-spin, strongly coupled Fe^{II}(bpy)$(DBSQ)_2$ species with an $S = 1$ spin state or to a diamagnetic low-spin Fe^{II}(bpy)$(DBSQ)_2$ isomer with strongly coupled radical ligands may contribute to this behavior.

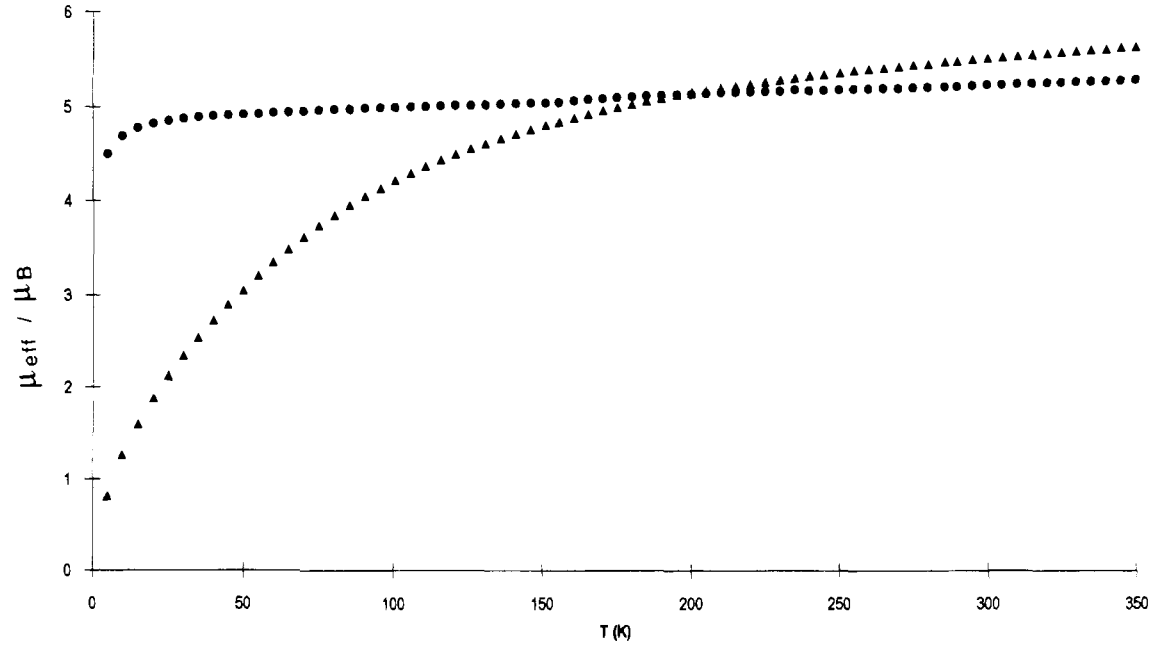

Figure 2. Plots of magnetic moment (μ_B) vs temperature (K) for Fe(bpy)(3,6-DBSQ)(3,6-DBCat) (▲) and Fe(tmeda)(3,6-DBSQ)(3,6-DBCat) (●).

Table 6. Electronic Spectral Data and Electrochemical Potentials for Members of the Fe(N-N)(DBSQ)(DBCat) Series[a]

compound	λ_{max}, nm (ϵ, M^{-1} cm^{-1})	$E_{1/2}$, V vs Fc/Fc^+ (ΔE_p, mV)
Fe(bpy)(3,6-DBSQ)(3,6-DBCat)	360 (3200), 450 (3100), 560 (3000), 710 (4100)	−0.34 (165), −0.84 (175), −2.06
Fe(tmeda)(3,6-DBSQ)(3,6-DBCat)	423 (3600), 446 (3400), 545 (3600), 790 (4000)	−0.26 (185), −0.84 (165), −1.96
Fe(tmeda)(3,5-DBSQ)(3,5-DBCat)	415 (4500), 447 (4400), 514 (4000), 575 (4200), 740 (5600)	−0.27 (132), −0.78 (131), −1.88
$Fe(py)_2$(3,6-DBSQ)(3,6-DBCat)[b]	413 (2400), 563 (1700), 835 (2000)	−0.34 (128), −0.86 (115), −1.42

[a] Electronic spectra recorded in dichloromethane. [b] Reference 6.

However, the Fe(II) charge distribution would be thermodynamically favored as the high-temperature isomer since both ΔH and ΔS for the Fe(III)/Fe(II) transition (eq 6) would be positive.[5] Further, the preliminary results of Mössbauer measurements fail to show evidence for a transition to Fe(II).[12] At 200 K ΔE_Q = 1.025 mm/s and δ = 0.396 mm/s, while at 110 K ΔE_Q = 1.054 mm/s and δ = 0.414 mm/s. The drop in magnetic moment with decreasing temperature appears to more likely result from intermolecular exchange propagated through the stacked bpy ligands. We note, however, that Mn(phen)(3,6-DBSQ)(3,6-DBCat) shows the same phen-stacked crystal structure but remains strongly paramagnetic with a magnetic moment greater than 3.5 μ_B at temperatures below 10 K.[3b]

Electronic spectra recorded on Fe(bpy)(3,6-DBSQ)(3,6-DBCat) showed a marked solvent dependence. In dichloromethane (Table 6), a band appears at 360 nm (ϵ 3200 M^{-1} cm^{-1}) as a shoulder on more intense bands between ligand-localized electronic levels that appear in the UV. The position of this transition is less dependent on solvent than bands at lower energy. Bands in three distinct spectral regions appear at lower energy. An unsymmetrical band appears at 450 nm (ϵ 3100) in CH_2Cl_2, and a band at 560 nm appears as a shoulder on an intense transition at 710 nm (ϵ 4100). This low-energy transition shows the greatest dependence on solvent, moving to higher energy and coalescing with the 560 nm transition in THF to give a single band at 570 nm and moving to lower energy to give two clear absorptions at 550 and 780 nm in toluene. This behavior appears similar to spectral observations on Fe(bpy)(3,5-DBSQ)(3,5-DBCat), where a low-energy transition was reported to appear at 640 nm in toluene, moving to 592 nm in THF. A band assigned as a Cat → Fe(III) CT transition commonly appears in this region for Fe^{III}(Cat) complexes.[13] A feature absent in the spectrum of Fe(bpy)(3,6-DBSQ)(3,6-DBCat) is a transition in the infrared. Both Co(bpy)(3,6-DBSQ)(3,6-DBCat) and Mn(bpy)(3,6-DBSQ)(3,6-DBCat) have transitions in the 2500 and 2100 nm regions, respectively.[2,3]

Electrochemical characterization of Fe(bpy)(3,6-DBSQ)(3,6-DBCat) shows two couples at −0.34 (165) and −0.84 (175) V (vs Fc^+/Fc) that correspond to SQ/Cat redox steps for the two quinone ligands. Compensation for cell *iR* drop shows that both couples are reversible. A broad reduction that appears near −2.0 V as a two overlapped irreversible one-electron process may be associated with bpy/bpy^- and Fe(III/II) reductions.[14] The two quinone redox couples appear at potentials that are shifted negatively from those of corresponding reduction steps of Fe(bpy)(Cl_4SQ)(Cl_4Cat) by roughly 0.8 V.[14] Resolution of the electrochemistry on Fe(bpy)(3,5-DBSQ)(3,5-DBCat) has been far more difficult,[14] but similarities in the magnetic and spectral properties of the two complexes prepared with the 3,6- and 3,5-DBQ ligands indicate that Fe(bpy)(3,5-DBSQ)(3,5-DBCat) is most likely monomeric in structure and similar to its 3,6-DBQ analog.

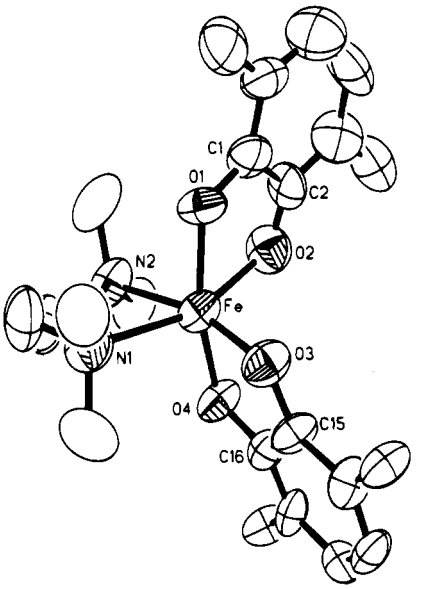

Figure 3. Drawing of Fe(tmeda)(3,6-DBSQ)(3,6-DBCat) with *tert*-butyl methyl carbon atoms omitted.

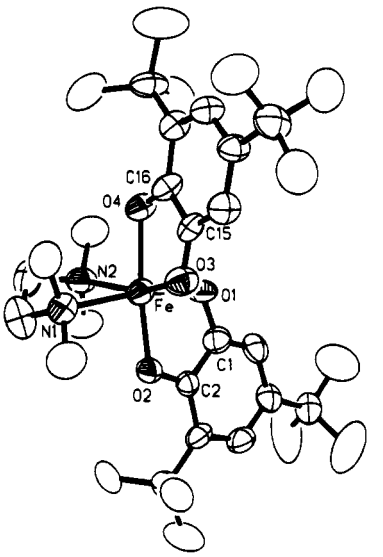

Figure 4. Drawing of Fe(tmeda)(3,5-DBSQ)(3,5-DBCat).

Fe(tmeda)(3,6-DBSQ)(3,6-DBCat) and Fe(tmeda)(3,5-DBSQ)(3,5-DBCat). Reactions carried out with $Fe(CO)_5$, tmeda, and either 3,6-DBBQ or 3,5-DBBQ have been found to give Fe(tmeda)(3,6-DBSQ)(3,6-DBCat) or Fe(tmeda)(3,5-DBSQ)(3,5-DBCat), respectively. Both complexes have been obtained in crystalline form and have been characterized structurally. Drawings of Fe(tmeda)(3,6-DBSQ)(3,6-DBCat) and Fe(tmeda)(3,5-DBSQ)(3,5-DBCat) appear in Figures 3 and 4; selected bond lengths and angles are listed in Table 5. In both structures, complex molecules are located at general positions of the space group with no imposed symmetry, and the features of the unique SQ and Cat ligands are clear.

(12) (a) Hendrickson, D. N. Research in progress. (b) Cohn, M. J.; Xie, C.-L.; Tuchagues, J.-P. M.; Pierpont, C. G.; Hendrickson, D. N. *Inorg. Chem.* **1992**, *31*, 5028.
(13) Jang, H. G.; Cox, D. D.; Que, L., Jr. *J. Am. Chem. Soc.* **1991**, *113*, 9200.
(14) Zirong, D.; Bhattacharya, S.; McCusker, J. K.; Hagen, P. M.; Hendrickson, D. N.; Pierpont, C. G. *Inorg. Chem.* **1992**, *31*, 870.

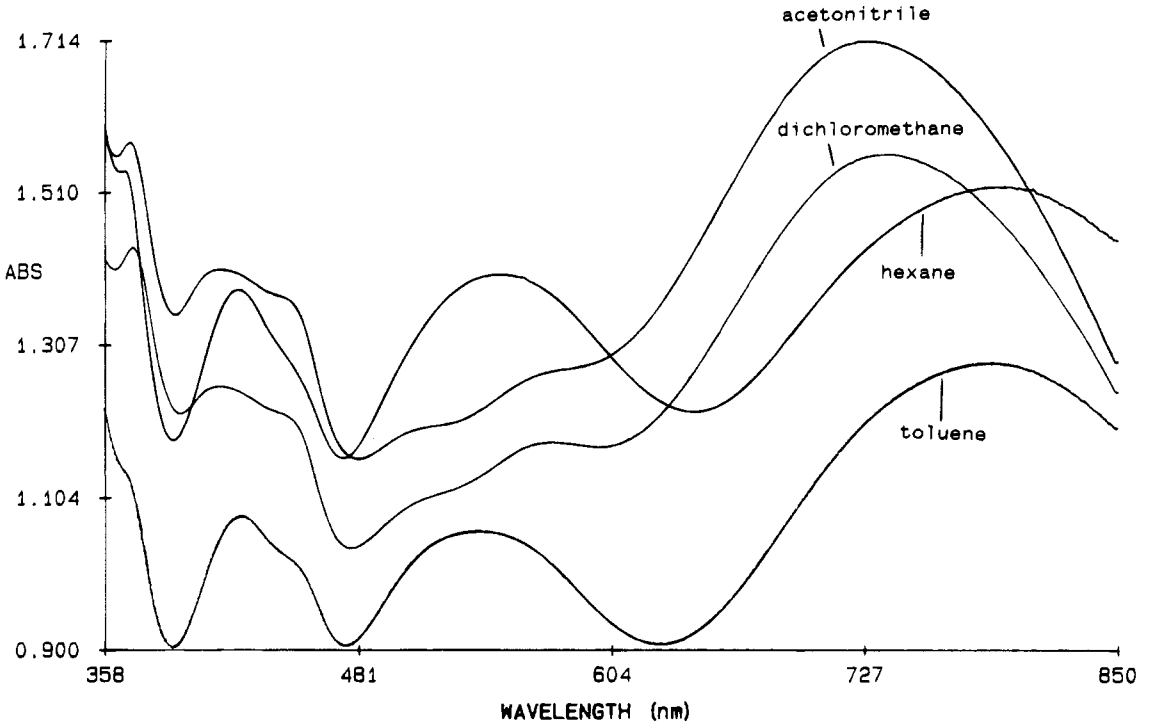

Figure 5. Electronic spectra of Fe(tmeda)(3,5-DBSQ)(3,5-DBCat) recorded in hexane, toluene, dichloromethane, and acetonitrile solutions [C = 3.3 × 10^{-4} M (hexane, DCM); C = 5.0 × 10^{-4} M (AN); C = 7.5 × 10^{-4} M (tol)].

Semiquinone ligands have average C−O lengths of 1.26(2) Å for Fe(tmeda)(3,6-DBSQ)(3,6-DBCat) and 1.28(1) Å for Fe(tmeda)(3,5-DBSQ)(3,5-DBCat). Catecholate ligands have longer C−O lengths of 1.35(2) and 1.34(1) Å for the two complexes. As a general feature, Fe−O_{Cat} lengths are shorter than Fe−O_{SQ} lengths, and the Fe−N lengths are longer than values of Fe(bpy)(3,6-DBSQ)(3,6-DBCat). The structure determination on Fe(tmeda)(3,5-DBSQ)(3,5-DBCat) was carried out with interest in determining whether the molecule is monomeric or oligomeric.[7] It is clearly a monomer, and in neither case are there close intermolecular contacts that might contribute to anomalous magnetic behavior. A plot of μ_{eff} vs T for Fe(tmeda)(3,6-DBSQ)(3,6-DBCat) is shown in Figure 2; the 3,5-DBQ analog shows similar behavior. The magnetic moment drops from 5.29 to 4.82 μ_B over the temperature range 350−20 K but drops more sharply to 4.50 μ_B at 5 K. There is no evidence for significant intermolecular exchange, in contrast with the behavior of Fe(bpy)(3,6-DBSQ)(3,6-DBCat).

Electronic spectra were recorded for both complexes in a variety of solvents. Spectra were also recorded at different temperatures, but little temperature dependence in band position was observed. Solvatochromic shifts were most striking for Fe(tmeda)(3,5-DBSQ)(3,5-DBCat), and solvent-dependent spectral changes are shown in Figure 5. Spectra recorded in nonpolar solvents (hexane, toluene) are markedly different from spectra obtained in acetonitrile and dichloromethane. Values for λ_{max} in hexane and toluene for the Cat → Fe(III) transition at lowest energy are 795 and 790 nm, respectively. This transition increases in energy to 740 nm to CH_2Cl_2 and 730 nm in acetonitrile. Related behavior has been noted for a similar transition of $[Fe^{III}(CTH)(3,5\text{-}DBCAT)]^+$.[15] A band that appears in the 540 nm region in nonpolar solvent spectra splits to give two separate bands at 510 and 575 nm in the polar solvent spectra. The higher energy component of the overlapped bands in the 400 nm region shifts from 425 nm in nonpolar solvents to 415 nm in the polar solutions while the 450 nm absorptions

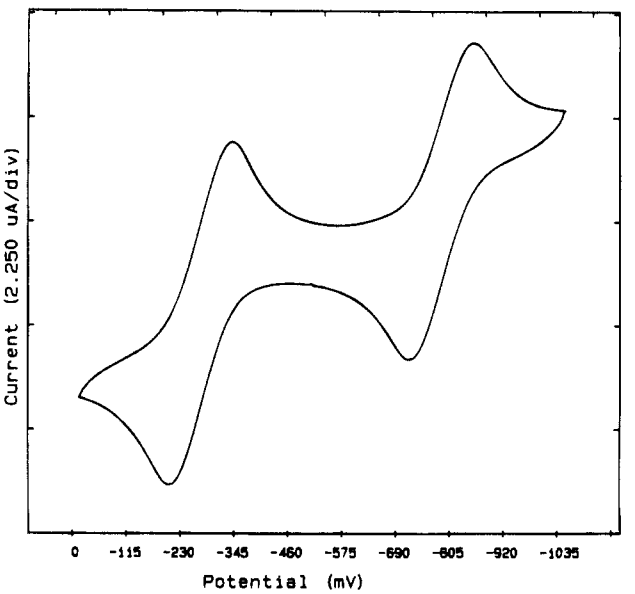

Figure 6. SQ/Cat redox couples of Fe(tmeda)(3,5-DBSQ)(3,5-DBCat) measured in dichloromethane at a scan rate of 100 mV/s.

remains unchanged. The assignment for the higher energy transitions in the 400 and 500 nm regions is unclear, but they appear for *trans*-Fe(py)$_2$(3,6-DBSQ)(3,6-DBCat) and are not directly associated with the nitrogen coligand.[6] Related bands appear for Fe(tmeda)(3,6-DBSQ)(3,6-DBCat) with λ_{max} values at 720, 515, 440, and 425 nm in acetonitrile shifted to 792, 545, 450, and 425 in toluene. Spectra recorded on $[Fe(CTH)(3,5\text{-}DBCat)]^+$ in acetonitrile also show an intense transition in the 530 nm region. Electrochemical characterization of Fe(tmeda)(3,5-DBSQ)(3,5-DBCat) and Fe(tmeda)(3,6-DBSQ)(3,6-DBCat) produced results that are similar to the CV of Fe(bpy)(3,6-DBSQ)(3,6-DBCat) (Table 6). Two quinone ligand SQ/Cat couples are observed (Figure 6), with an irreversible Fe(III/II) couple appearing at more negative potentials.

(15) Dei, A. *Inorg. Chem.* **1993**, *32*, 5730.

Discussion

The results of characterization of the three complexes of general structure Fe(N-N)(DBSQ)(DBCat) show that the complexes of 3,6- and 3,5-DBQ are both monomeric and similar in structure as complexes of Fe(III) with mixed-charge SQ and Cat ligands. Their magnetic properties indicate that the $S = {}^5/_2$ Fe(III) center is coupled antiferromagnetically with the $S = {}^1/_2$ radical SQ ligand. An anomalous drop in magnetic moment with decreasing temperature observed for Fe(bpy)(3,6-DBSQ)-(3,6-DBCat) appears to be associated with intermolecular coupling through bpy ligands of adjacent molecules in the stacked crystal structrure of the complex. Electrochemistry consists of oxidation and reduction couples that occur at the quinone ligands, with irreversible reduction occurring at the metal at more negative potentials. In contrast to the electronic spectra of related complexes of cobalt and manganese which show temperature dependence associated with equilibria between redox isomers, electronic spectra of the Fe(N-N)(DBSQ)-(DBCat) series show little temperature dependence but strong solvent dependence. Further, the intense, low-energy transitions of Co(N-N)(DBSQ)(DBCat) and Mn(N-N)(DBSQ)(DBCat) that appear in the infrared are not observed for members of the iron series with chelating N-donor coligands. Since electronic coupling between the SQ and Cat ligands is probably not markedly different in the iron complexes, the transitions observed with Co and Mn are probably not intervalence transitions between the quinone ligands of mixed charge.

The Absence of Redox Isomerism for the Fe(N-N)(DBSQ)-(DBCat) Series. Equilibria between redox isomers observed for related complexes of Co and Mn are not observed for members of the Fe(N-N)(DBSQ)(DBCat) series. This may be understood from consideration of the thermodynamic changes that contribute to the equilibria of the Co and Mn series.[4] For both metal ions, intramolecular changes in enthalpy and entropy are large and positive for the equilibria described in eqs 2 and 3 and eqs 4 and 5. Values have been determined directly for Co(bpy)(3,5-DBSQ)(3,5-DBCat) from equilibrium measurements in toluene solution and for solid samples. A relatively large enthalpy change is associated with the decrease in metal bond energies accompanying the transition from low-spin Co(III) to high-spin Co(II). The similarity of ΔH values (ΔH_{soln} = 34 kJ mol^{-1}, ΔH_{solid} = 32 kJ mol^{-1}) obtained in solution and in the solid state indicates that solvation effects are relatively small, as might be expected with the *tert*-butyl-substituted quinone ligand. It should be noted that isomerism has not been observed for Co complexes prepared with the more exposed 9,10-phenanthrenequinone ligand where intermolecular contributions are more significant.[16] The large positive entropy change associated with equilibria of the cobalt complexes (ΔS_{soln} = 125 J mol^{-1} deg^{-1}, ΔS_{solid} = 98 J mol^{-1} deg^{-1}) results primarily from a low-energy shift in vibrational modes, the increase in spin degeneracy that accompanies the change in charge distribution and metal spin state, and the structural flexibility of the M(II) isomers in solution. Similar changes in metal−ligand bonding and complex spin multiplicity are associated with the transition from Mn(IV) to high-spin Mn(II), and the two-step equilibria observed for members of the Mn(N-N)(DBQ)$_2$ series result from related thermodynamic contributions. The observation that members of the iron series fail to show valence tautomeric equilibria is in agreement with this model. Richardson has related the magnitude of intramolecular entropy changes in metal redox processes to changes in the composition of dσ orbitals; the addition of charge to the antibonding octahedral e_g level results in a large entropy increase.[5] Reduction of high-spin Fe(III) to high-spin Fe(II) would result in a decrease in metal−ligand bond energies, an increase in Fe−L bond lengths, and an increase in ΔH. But the enthalpy change would be far smaller for the Fe(III/II) reduction than the large changes associated with the Co(III/II) and Mn(IV/II) reductions. Fe−O bonds to the protonated catecholate ligands of Fe^{III}(OPPh$_3$)$_3$(Cl$_4$Cat)(H−Cl$_4$Cat) and [Fe^{II}(6TLA)(H−3,5-DBCat)]$^+$ differ by 0.03 Å,[14,17] while Co(III/II) and Mn(IV,II) bond length changes are roughly 0.2 Å. A positive entropy increase may be expected for the reaction described in eq 6, but it too will be far smaller in magnitude than the ΔS values of the Co and Mn redox couples. Richardson has estimated that $\Delta S_{vib}°$ is 15.5 J mol^{-1} deg^{-1} for the $FeCl_4^{-/2-}$ couple, compared with 62.3 J mol^{-1} deg^{-1} for the $[Co(NH_3)_6]^{3+/2+}$ couple.[5b] With antiferromagnetic Fe−SQ exchange, $\Delta S_{elec}°$ for the Fe^{III}(Cat)/Fe^{II}(SQ) change in charge distribution would be small or possibly negative. As a result, the intramolecular electronic and vibrational thermodynamic changes that contribute significantly to the Co and Mn equilibria are far smaller with Fe, and differential solvation effects become more significant, as is apparent from the strong solvatochromism observed for the Fe(N-N)(DBSQ)(DBCat) series.

Acknowledgment. We thank Professor G. A. Abakumov for providing the sample of Fe(bpy)(3,6-DBSQ)(3,6-DBCat) used in initial characterization experiments. We also thank Brenda Conklin for recording magnetic susceptibility measurements, Professor M. F. El-Shahat of Ain Shams University for helpful comments, and Professor Lawrence Que, Jr., for providing a copy of ref 17 prior to publication. Support for this research was provided by the National Science Foundation through Grant CHE 90-23636 and the Egyptian Ministry of Science in the form of a Graduate Fellowship for A.S.A.

Supporting Information Available: Tables giving crystal data and details of the structure determination, atomic coordinates, anisotropic thermal parameters, hydrogen atom locations, and bond lengths and angles for Fe(bpy)(3,6-DBSQ)(3,6-DBCat), Fe(tmeda)(3,6-DBSQ)(3,6-DBCat), and Fe(tmeda)(3,5-DBSQ)(3,5-DBCat) (36 pages). Ordering information is given on any current masthead page.

IC9501475

(16) Lynch, M. W.; Buchanan, R. M.; Pierpont, C. G.; Hendrickson, D. N. *Inorg. Chem.* **1981**, *20*, 1038.

(17) Chiou, Y.-M.; Que, L., Jr. *Inorg. Chem.*, submitted for publication.